

## Experimental research on load-bearing capacity of cast steel joints for beam-to-column

Qinghua Han<sup>1,2a</sup>, Mingjie Liu<sup>1</sup> and Yan Lu<sup>\*1,2</sup>

<sup>1</sup>School of Civil Engineering, Tianjin University, Tianjin 300072, China

<sup>2</sup>Key Laboratory of Coast Civil Structure Safety of China Ministry of Education, Tianjin University, Tianjin 300072, China

(Received December 24, 2014, Revised March 24, 2015, Accepted September 15, 2015)

**Abstract.** The load transfer mechanism and load-bearing capacity of cast steel joints for H-shaped beam to square tube column connection are studied based on the deformation compatibility theory. Then the monotonic tensile experiments are conducted for 12 specimens about the cast steel joints for H-shaped beam to square tube column connection. The findings are that the tensile bearing capacity of the cast steel joints for beam-column connection depends on the ring of cast steel stiffener. The tensile fracture happens at the ring of the cast steel stiffener when the joint fails. The thickness of square tube column has little influence on the bearing capacity of the joint. The square tube column buckles while the joint without concrete filled, but the strength failure happens for the joint with concrete filled column. And the length of welding connection between square tube column and cast steel stiffener has little influence on the load-bearing capacity of the cast steel joint. Finally it is shown that the load-bearing capacity of the joints for H-shaped beam to concrete filled square tube column connection is larger than that of the joints for H-shaped beam to square tube column connection by 10% to 15%.

**Keywords:** square tube column; cast steel joints; monotonic tensile experiment; load transfer mechanism; load-bearing capacity

### 1. Introduction

Square tube column and H-shaped beam frame structure is one type of steel frame structures. The geometrical characteristics of square tube in the two directions are the same, so its mechanical properties in any directions are identical, makes the square tube column a better choice for the frame column than the H-shaped column. At present, the H-shaped beam and square tube column frame structure is widely used in multi-story and high-rise steel frame structure (Skejic *et al.* 2008). When the load transfers, frame joint is the key part connecting beams with columns. The joint makes great influence on the bearing capacity of the beams and column of the frames. The mechanical performance of the frame joint has great effect on the structural behavior of the steel frame structure (Shin *et al.* 2008, Ciutina and Dubina 2006).

---

\*Corresponding author, Ph.D., E-mail: yanlu86@tju.edu.cn

<sup>a</sup>Professor, E-mail: qhhan@tju.edu.cn

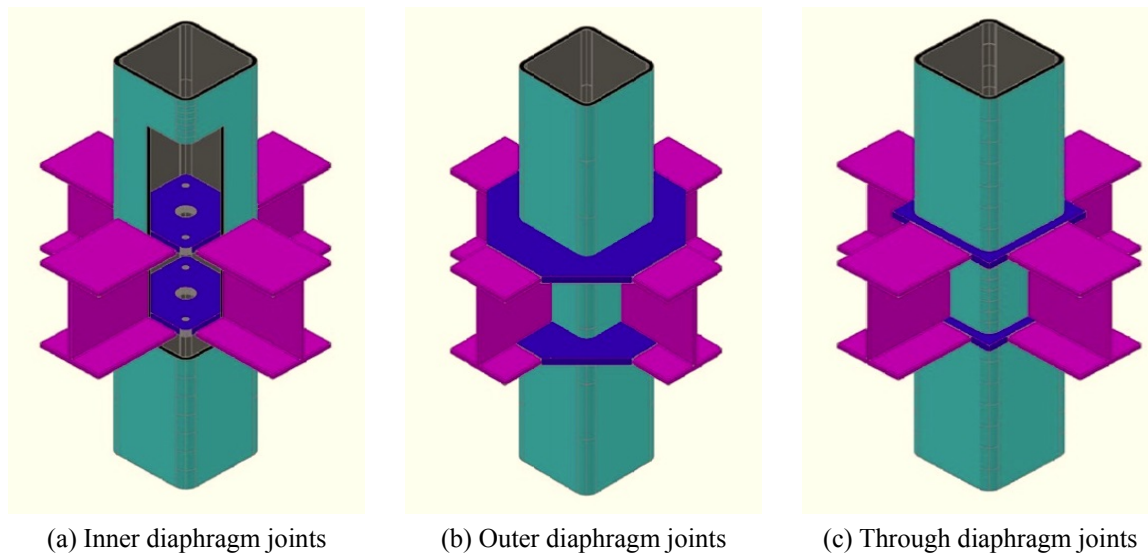


Fig. 1 Common joints

Since the square tube column has sealed section, the construction of the joint for H-shaped beam to square tube column connection has great difference with the joint for H-shaped beam to H-shaped column. In general, the joint without the stiffener has lower bearing capacity than the joint with the stiffener for H-shaped beam to square tube column connection. In order to improve the bearing capacity of the frame joint, the stiffener should be added to the joint for H-shaped beam to square tube column connection. The common joints around the world include the joints with inner diaphragm, joints with outer diaphragm and joints with through diaphragm (Morino and Tsuda 2003). The construction of those joints is shown in Fig. 1. Firstly, steel plate or section steel are cut into several parts, then those parts are added to steel tube column as the stiffeners by welding, finally the joint with the stiffener are formed, while much time and money are taken to form the joints. The processing work is complex and difficult. Meanwhile, the welding seam may be close to each other or even crossing. A large welding heat affected zone will appear and affect the mechanical properties of the joints.

To improve the behaviour of steel frame structure, several kinds of novel beam-column joints were studied. Kimura *et al.* (2005) studied the beam-column connection joint with the vertical stiffener by test. It was found that the joint with vertical stiffeners had sufficient capacities over the full plastic strength of beams. Wang and Zhang (2009) preceded an experimental program for bolted moment connection joints using high-strength blind bolts. The blind bolted connection was shown to be a reliable and effective solution for moment-resisting composite frame structures by test. Toellner *et al.* (2015) conducted a set of twelve full-scale moment connection tests to explore the seismic behavior of steel moment connections with decking attachments. All twelve specimens were proved to have qualified moment bearing capacity, energy dissipation capacity.

In order to simplify the construction and improve the mechanical performance of the joint, cast steel joints for H-shaped beam to square tube column connection were appeared in Japan (in Fig. 2). In this novel joint, cast steel stiffener is used as the stiffener to transfer the internal force of the beams and columns and formed into beam-column connection. The cast steel stiffener is mainly

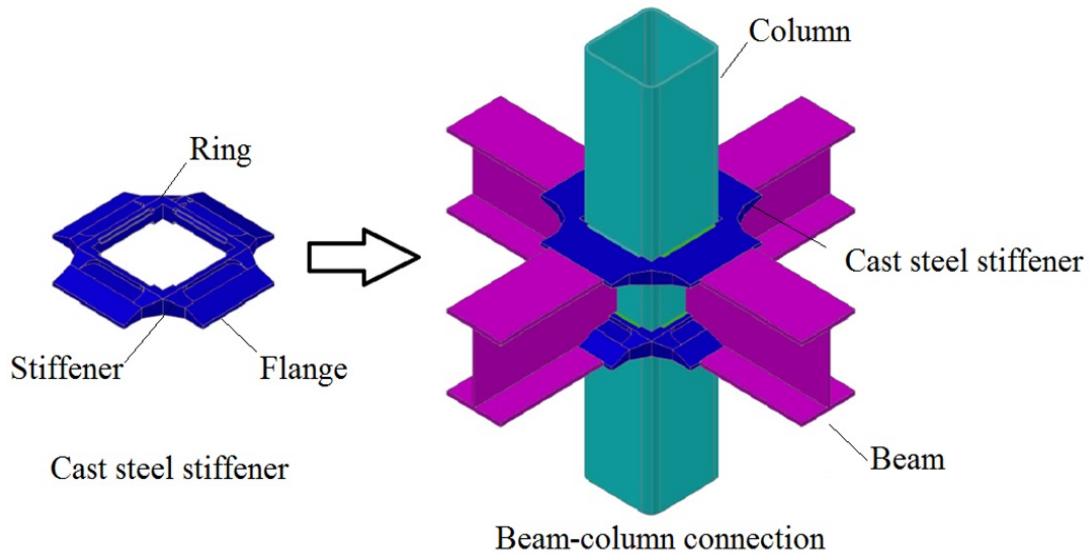


Fig. 2 Cast steel stiffener and cast steel joints for beam-column connection

composed of the ring connected with the square tube column, the flange connected with the beam and the stiffener connected with the ring and the flange. There are two cast steel stiffeners to connect the beam into the column. First, the cast steel stiffeners are installed around the tube column according to the position of beam flange. Then, the beam flange is connected with the flange of cast steel stiffener by butt welding and the web plate of the beam is connected with the tube column by fillet welding. Eight precast grooves are set in the top and bottom surface of the four sides of cast ring. The cast steel stiffener is connected to columns by partial penetration butt weld along precast grooves. There is no weld at the round-corner of the square tube column to reduce the stress concentration of the column.

The advantages of this joint is simple construction, little welding heat effect, good mechanical performance and convenient fabrication procedure (Design code of Hitachi 2001). At present, there were several researches about cast steel joints for beam-column connection. Nakano *et al.* (2003) conducted monotonic tensile experimental research on the load-bearing capability of cast steel joints without filled concrete when the forms of cast steel stiffeners are different. Research showed that cast steel stiffener will improve the load-bearing capacity. The load-bearing capacity formula based on yield line theory was derived. However, it did not validate the load transfer path by test. Han *et al.* (2015) presented load-bearing capacity theory and formula based on the deformation compatibility condition. This paper conduct a monotonic tensile experimental research on the load transfer mechanism and load-bearing capacity of cast steel joints for H-shaped beam to square tube column connection. Research focus on the influence factors on load-bearing capability of joints such as the size of square tube column and cast steel stiffeners and the concrete filled in the tube, validation of the load-bearing capacity theory based on the deformation compatibility condition.

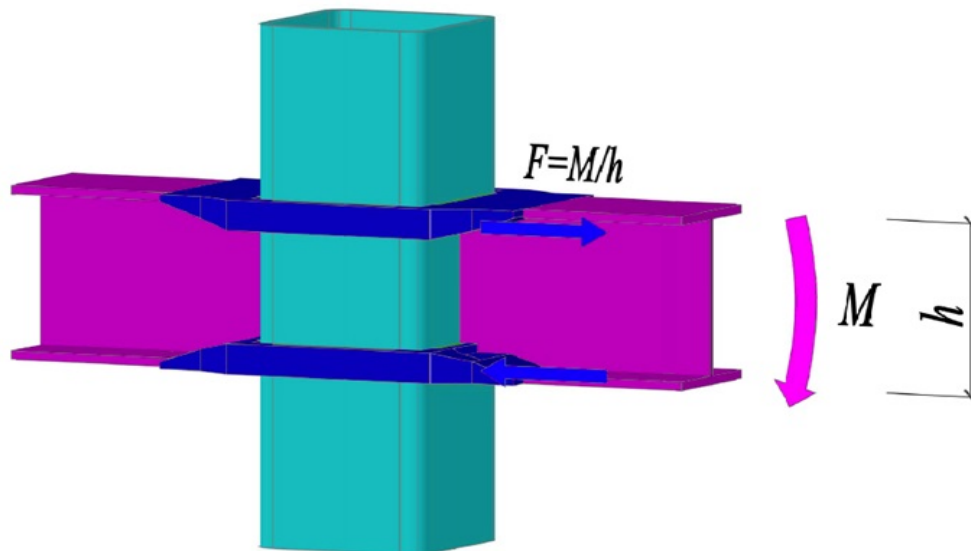


Fig. 3 Load transfer path

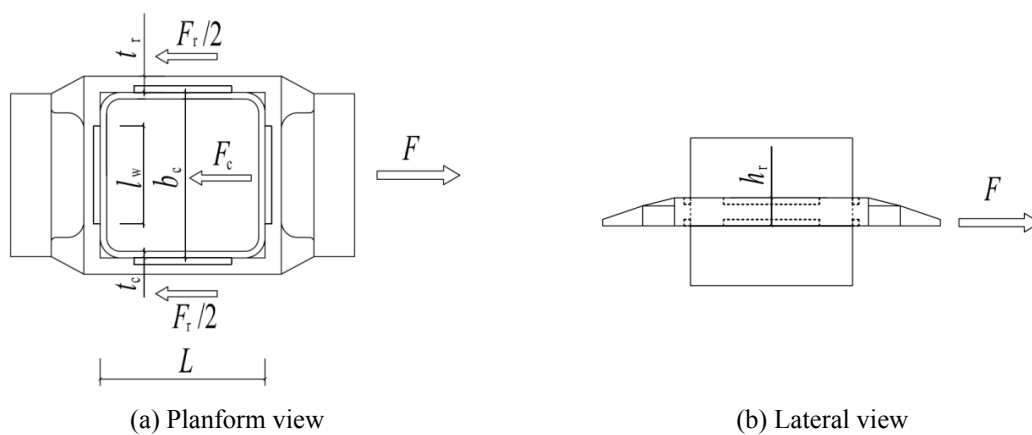


Fig. 4 The load transfer mechanism

## 2. Load-bearing capacity of cast steel joints for H-shaped beam to square tube column connection

### 2.1 Load-bearing capacity theory based on the deformation compatibility condition

When the joint for beam-column connection bears the bending moment  $M$ , the bending moment  $M$  transforms to the tensile force  $F$  on the stiffener. The load transfer path is shown in Fig. 3.

Based on the load transfer path, the load-bearing capacity of cast steel joints depends on the tensile bearing capacity of the cast steel stiffener. The tensile force on the cast steel stiffener will be transferred to the ring of the stiffener and the square tube column wall through the flange of the stiffener. Then the ring of the stiffener and the square tube column wall will bear the tensile force

together. The load transfer mechanism is shown in Fig. 4 and Eq. (1).

$$F = F_r + F_c \quad (1)$$

in which  $F$  is the tensile force on the flange of stiffener,  $F_r$  is the tensile force on the ring of stiffener.  $F_c$  is the tensile force on square tube column.  $t_r$  is the thickness of the ring of stiffener.  $t_c$  is the thickness of square tube column wall.  $l_w$  is length of welding connection between square tube column and cast steel stiffener.  $L$  is the length of the ring of stiffener.  $b_c$  is the length of the side of square tube column.  $h_r$  is the height of the ring of stiffener.

In order to acquire the force distribution in the joint, the load-bearing capacity theory based on the deformation compatibility condition was presented by Han *et al.* (2015). It shows that the ring of stiffener and the square tube column wall have the equal deformation under the tensile force. The tensile force on the ring of stiffener and the square tube column is proportional to the tensile stiffness of those as shown in Eq. (2).

$$\frac{F_r}{F_c} = \frac{K_r}{K_c} \quad (2)$$

where  $K_r$  is the tensile stiffness of the ring of stiffener,  $K_c$  is the tensile stiffness of square tube column wall.

The tensile deformation of the ring of stiffener  $\Delta$  under the tensile force  $F_r$  can be obtained from Eq. (3)

$$\Delta = \frac{F_r / 2}{EA} L \quad (3)$$

where  $A$  is the sectional area of the ring of stiffener.  $E$  is the elasticity modulus of steel.

The tensile stiffness of the ring of stiffener  $K_r$  can be obtained from Eq. (4).

$$K_r = \frac{F_r}{\Delta} = \frac{2EA}{L} \quad (4)$$

Then the square tube column wall under the tensile force load can be modeled as a four-edge supported plate under uniform line load at mid-span. It is difficult to acquire the solution of deformation. Finally it is simplified as a four-edge supported plate under concentrated force at mid-span. The deformation of the square tube column wall  $\Delta$  under the tensile force  $F_c$  can be obtained from Eq. (5).

$$\Delta = 0.0056 \frac{F_c b_c^2}{D} \quad (5)$$

where  $D$  is the flexural rigidity of plate per unit width.  $D$  can be obtained from Eq. (6) (Timoshenko and Woinowsky-Krieger 1959).

$$D = \frac{Et_c^3}{12(1 - \mu^2)} \quad (6)$$

where  $\mu$  is the Poisson ratio of steel.

Then the tensile stiffness of square tube column wall  $K_c$  can be obtained from Eq. (7).

$$K_c = \frac{F_c}{\Delta} = \frac{Et_c^3}{0.0611b_c^2} \quad (7)$$

Substituting Eq. (4) and Eq. (7) into Eq. (2), the ratio of the tensile force applied on the ring of stiffener  $F_r$  and square tube column wall  $F_c$  is shown in Eq. (8).

$$\frac{F_r}{F_c} = \frac{0.1222Ab_c^2}{Lt_c^3} \quad (8)$$

The tensile stress of the ring of stiffener  $\sigma_r$  under the tensile force  $F_r$  can be obtained from Eq. (9).

$$\sigma_r = \frac{F_r}{2A} \quad (9)$$

By the theory of plates and shells, the distributed bending moment  $M_y$  at the edge of a four-edge supported plate under concentrated force  $F_c$  at mid-span can be obtained from Eq. (10)(Timoshenko and Woinowsky-Krieger 1959). And the stress of square tube column wall  $\sigma_c$  under tensile force  $F_c$  can be obtained from Eq. (11).

$$M_y = 0.1257F_c \quad (10)$$

$$\sigma_c = 4\frac{M_y}{t_c^2} = 0.5028\frac{F_c}{t_c^2} \quad (11)$$

Substituting Eq. (9) and Eq. (11) into Eq. (2), the ratio of the stress for the ring of stiffener  $\sigma_r$  and square tube column wall  $\sigma_c$  is shown in Eq. (12).

$$\frac{\sigma_r}{\sigma_c} = \frac{0.1215b_c^2}{Lt_c} \quad (12)$$

## 2.2 Load transfer mechanism and load-bearing capacity formula of joints

In order to study the load transfer mechanism and force distribution in the joints, theoretical analysis is conducted. The geometrical parameters of the joints and the ratio of the tensile force of square tube column wall and the ring of stiffener ( $F_c/F_r$ ) and the stress of those ( $\sigma_c/\sigma_r$ ) are counted and listed in Table 1.

From Table 1, the tensile force on square tube column wall  $F_c$  is much less than that on the ring of stiffener  $F_r$  and the stress of square tube column wall  $\sigma_c$  is less than that of the ring of stiffener  $\sigma_r$ . However, the ratio of the yield stress of Q235B (mostly used as section steel for building in China) steel and ZG230-450 (mostly used as cast steel joint for building in China) cast steel is 1.022. The finding is that the ring of cast steel stiffener bears most of load transferred by the joint.

Table 1 The force distribution of the joints

$t_c$ (mm)	$b_c$ (mm)	$t_r$ (mm)	$h_r$ (mm)	$F_c/F_r$	$\sigma_c/\sigma_r$
4				0.00374	0.165
5	200	20	35	0.00731	0.206
6				0.0126	0.247
8				0.0299	0.329

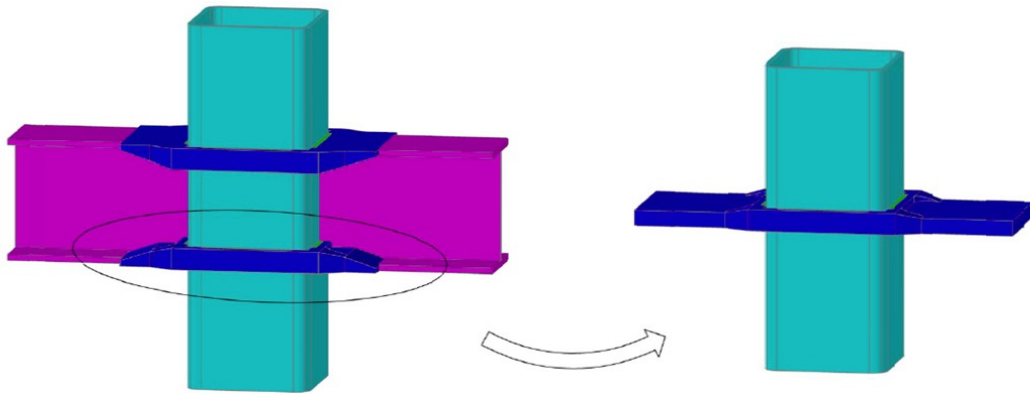


Fig. 5 Experimental specimen

The load-bearing capacity of cast steel joint depends on the tensile capacity of the ring of stiffener. Then the load-bearing capacity of the cast steel joint  $P$  is simplified as Eq. (13) (Han *et al.* 2015).

$$P = 2t_r h_r f_{yr} \tag{13}$$

where  $f_{yr}$  is the yield stress of cast steel.

### 3. Monotonic tensile experiments

In order to study the load transfer mechanism and obtain the load-bearing capacity of the joints, 12 specimens are designed for the monotonic tensile experiment. The monotonic tensile experimental specimen only includes one piece of cast steel stiffener and the square tube column connected with the stiffener without considering the effect of beam-end (Rong *et al.* 2013).

#### 3.1 Specimen layout and test setup

To avoid the beam flange buckle and the weld between beam flange and flange of cast steel stiffener damage, the extended flange of cast steel stiffener is fixed in the tensile testing machine. The details of the specimen are shown in Fig. 6. 12 test specimens consist of the square tube column and the cast steel stiffener. The experimental parameters of specimen are shown in Table 2.

Table 2 Specimen parameters

Specimen	Square tube column ( $b_c \times t_c$ ) (mm)	Connection between square tube column and cast steel stiffener	$l_w$ (mm)	Concrete filled in tube
1	200×4			
2	200×5	partial penetration butt weld	150	None
3	200×6			
4	200×8			
5	200×8			
6	200×6	fillet weld	100	
7			50	
8			10	
9			200×4	
10	200×5	partial penetration butt weld	150	C30
11	200×6			
12	200×8			

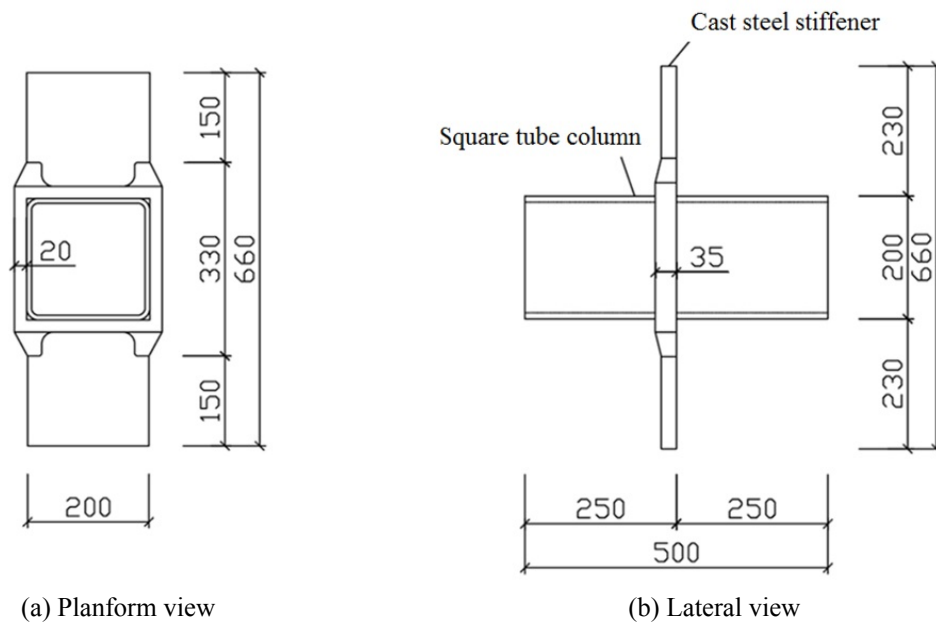


Fig. 6 Specimen layout

The steel of square tube column and the cast steel stiffener are respectively Q235B and ZG230-450 (Yin *et al.* 2009). The concrete filled in the tube is C30 (Yin *et al.* 2009). The material performance of steel and concrete is shown in Table 3 and Table 4.

The monotonic tensile test is conducted in the Building Materials Laboratory of Tianjin University. In order to simulate that the joint bears the bending moment, the tensile force is applied on the fixed end of specimen by the tensile testing machine. The test setup is shown in Fig. 7. The

Table 3 Material performance of steel

Steel material	Thickness (mm)	$f_y^*$ (N/mm <sup>2</sup> )	$f_u$ (N/mm <sup>2</sup> )	Elongation (%)
ZG230-450	-	353.9	527.3	26.9
Q235B	4	265.4	370.8	21.3
	5	311.5	437.3	25.3
	6	325.6	425.6	28.7
	8	317.9	437.9	29.3

\* $f_y$  is the measured yield strength.  $f_u$  is the measured ultimate strength.

Table 4 Material performance of concrete

Concrete material	$f_{cu,100}^*$ (N/mm <sup>2</sup> )	$f_{cu,150}$ (N/mm <sup>2</sup> )
C30	45.1	42.8

\* $f_{cu,100}$  is the measured average compressive strength of 100mm cubic.  $f_{cu,150}$  is the measured average compressive strength of 150mm cubic.



Fig. 7 Test setup

Table 5 Test result

Specimen	Yield load*(kN)	Ultimate load (kN)	Failure phenomena
1	477.3	526.7	tensile failure of the ring of stiffener & buckling of the square tube column wall
2	508.2	536.1	
3	532.0	685.0	
4	550.4	616.1	tensile failure of the ring of stiffener & crack at the edge of the weld connection between square tube column and cast steel stiffener
5	528.3	711.0	
6	534.1	734.9	
7	517.4	716.0	tensile failure of the ring of stiffener & the weld connection between square tube column and cast steel stiffener pulled apart
8	502.9	631.1	
9	532.9	645.0	tensile failure of the ring of stiffener & the square tube column wall tear apart
10	575.2	662.9	tensile failure of the ring of stiffener & buckling of the square tube column wall
11	594.6	707.9	tensile failure of the ring of stiffener & crack at the edge of the weld connection between square tube column and cast steel stiffener
12	631.7	714.5	

\*The yield load is defined by plotting method (Wang *et al.* 2013).

loading process is controlled by load at the beginning, the loading speed was 100kN each 5 minutes. The loading process is controlled by displacement after a turning point appears in the load-displacement curve till the specimen fails, the loading speed was 1.5 mm each 5 minutes during control by load. Every step of load would be hold for at least 3 minutes.

### 3.2 Experimental phenomena and result

The load-bearing capacity and failure modes of each specimen are listed in Table 5. The typical failure modes and the load-displacement curves are shown in Figs. 8 and 9. The key parameters in a typical load-displacement curve relationship of connection are shown in Fig. 10. For each specimen, when the load-displacement curve reaches the yield point, the ring of stiffener has great tensile stress, but the square tube column wall does not. When the tensile stress of the ring of stiffener continues to increase, the square tube column wall begins to curve. Finally the ring of stiffener fails under tensile force, as shown in Fig. 8(a). The failure mode of the square tube column wall is different due to the thickness of square tube column. When the thickness of square tube column is 4-5mm, it shows that square tube column wall bulges. And there is no significant failure at the weld connection between square tube column and cast steel stiffener. When the thickness of square tube column is 6-8mm, the bulge of the square tube column wall is slighter than that of the specimen for which the thickness of square tube column is 4-5 mm. Crack appears at the edge of the weld connection between square tube column and cast steel stiffener. When the length of the weld connection between square tube column and cast steel stiffener changes, the curve occurs for the square tube column wall. The crack in the weld connection between square tube column and cast steel stiffener happens in the edge when the length of the weld is 100 mm or 150 mm, as shown in Fig. 8(b). However the weld connection will pull apart when the length of the weld is 10 mm or 50 mm, as shown in Fig. 8(c). When the square tube is filled with concrete,

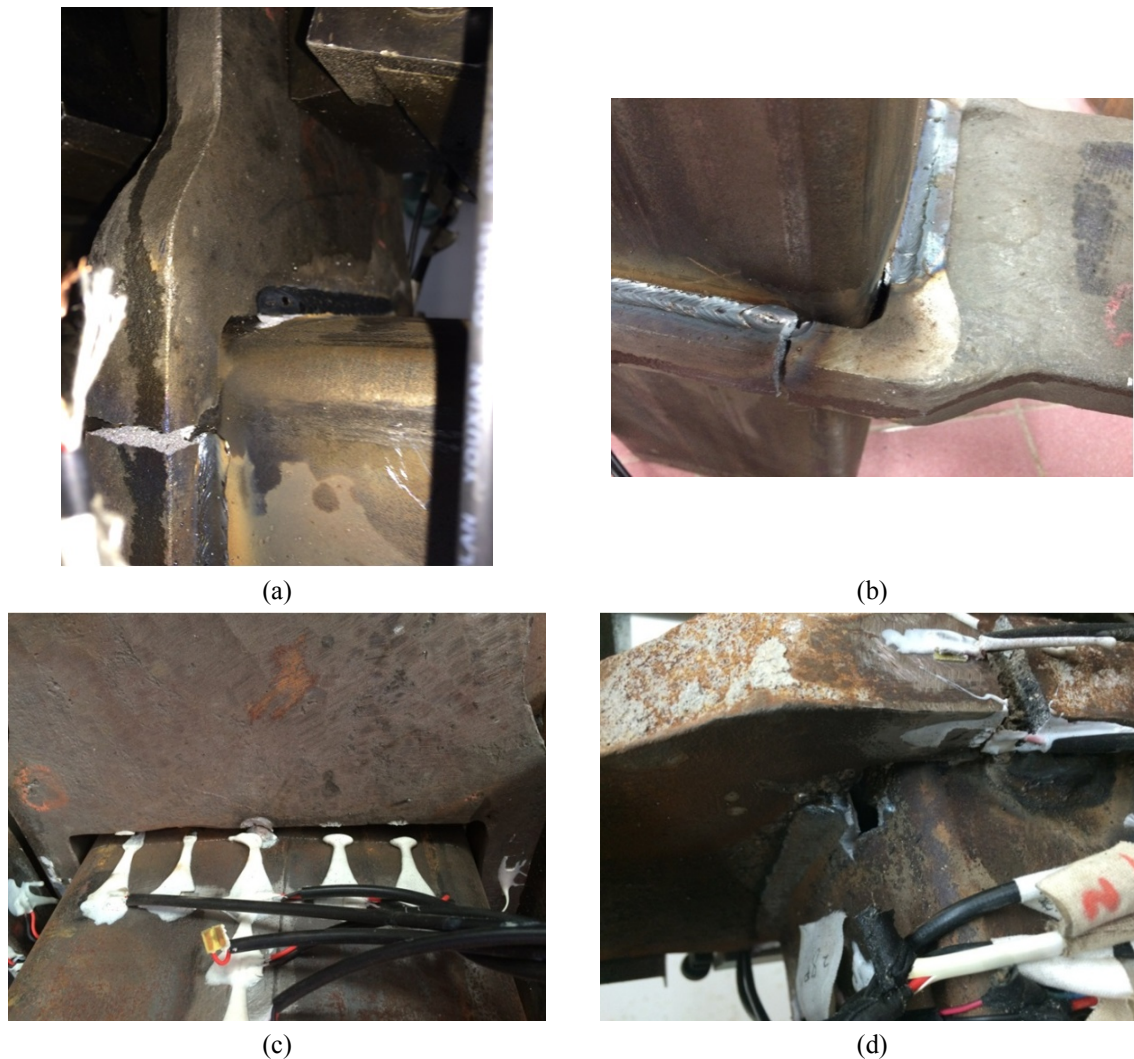


Fig. 8 Failure modes

- (a) tensile failure of the ring of stiffener & buckling of the square tube column wall (specimen 1),
- (b) tensile failure of the ring of stiffener & crack at the edge of the weld connection (specimen 4)
- (c) failure of weld connection between square tube column and cast steel stiffener (specimen 8)
- (d) tensile failure of the ring of stiffener & the square tube column wall tear apart (specimen 9)

the square tube column wall is split apart when the square tube column is thin such as Specimen 9, as shown in Fig. 8(d). There is no significant failure at the weld connection between square tube column and cast steel stiffener. The square tube column wall buckles when the thickness of the square tube column is 5-8 mm. There is crack in the edge of the weld connection between square tube column and cast steel stiffener.

The key parameters in a typical load-displacement curve relationship are shown in Fig. 10. The ultimate load  $P_u$  is defined by the maximum value of the test results. The yield load  $P_y$  is defined

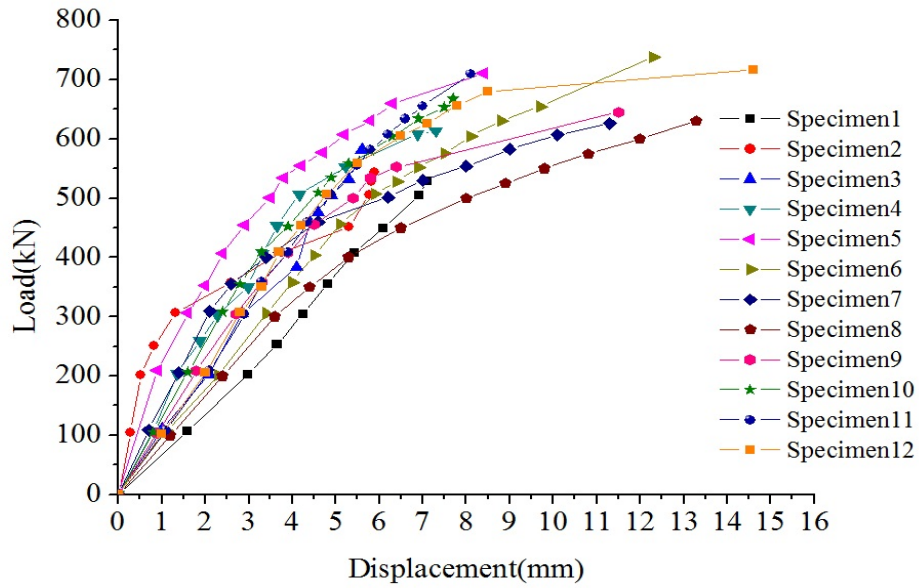


Fig. 9 Load-displacement curve

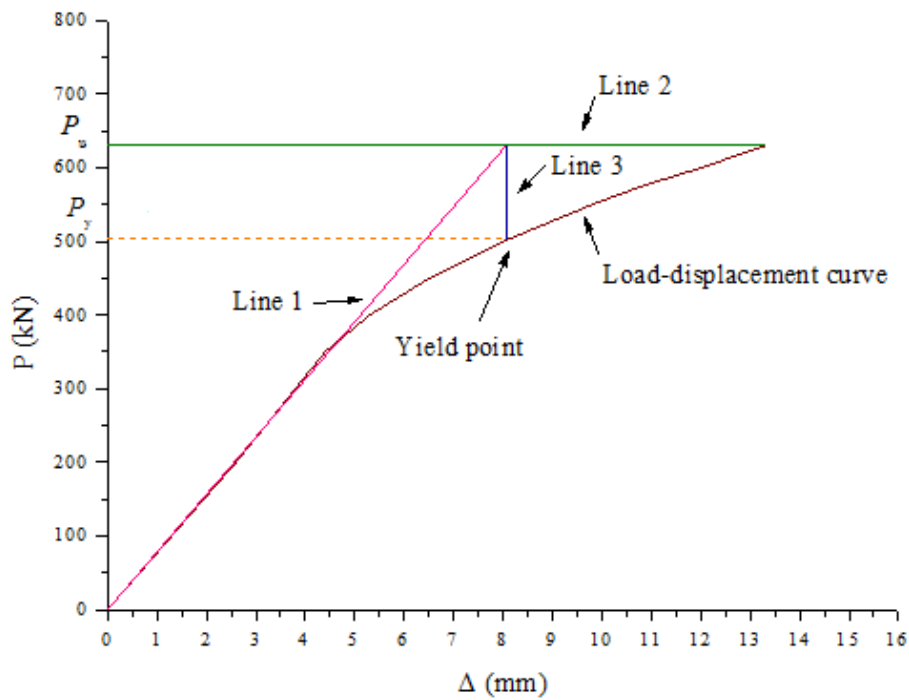


Fig. 10 Key parameters in a typical load-displacement curve relationship

by plotting method (Wang *et al.* 2013). Line 1 is drawn from original point with the slope of the load-displacement curve. Line 2 is drawn from the maximum value point of the load-displacement

curve and parallel with the  $X$ -axis. Line 3 is drawn from the intersection point of Line 1 and Line 2 and parallel with the  $Y$ -axis. The intersection point of Line 3 and load-displacement curve is the yield point and the load of the yield load  $P_y$  is defined by the load of yield point.

#### 4. Test analysis

##### 4.1 Load-bearing capacity of the cast steel joint

The load-bearing capacity of specimens is listed in Figs. 11 and 12 and Tables 6-7. It shows that the load-bearing capacity increases with the increase of thickness of the column for Specimen 1 to Specimen 4. When the thickness of the square tube column is same and the length of the weld connection between square tube column and cast steel stiffener is different, the load-bearing capacity seems to be same (from 502.9 kN to 534.1 kN). From Fig. 11, the finding is that the bearing capacity of the joint with concrete filled is higher from the joint without concrete filled. And the load-bearing capacity also increases with the increase of thickness of the column. It also shows that the different way of connection between square tube column and cast steel stiffener has little impact on the load-bearing capacity of the joint. It confirms that the simplified model for the wall of square tube column as a four-edge supported plate under concentrated force at mid-span is

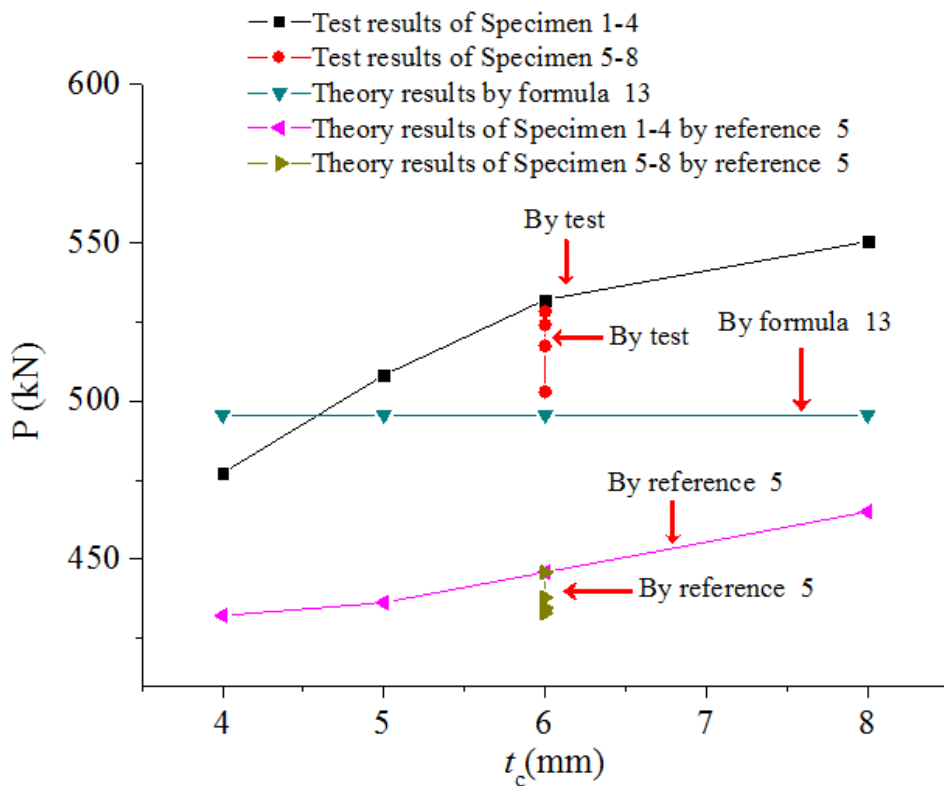


Fig. 11 Load-bearing capacity of specimen without filled concrete

Table 6 Comparison of the load-bearing capacity of specimen without filled concrete

Specimen	$P_1^*$ (kN)	$P_2$ (kN)	$P_3$ (kN)	$P_1/P_2$	$P_1/P_3$
1	477.3		432.2	0.963	1.104
2	508.2		436.3	1.025	1.165
3	532.0		445.9	1.073	1.193
4	550.4	495.6	465.0	1.111	1.184
5	528.3		445.9	1.066	1.185
6	534.1		437.9	1.078	1.220
7	517.4		434.6	1.044	1.191
8	502.9		433.0	1.015	1.162

\* $P_1$ ,  $P_2$ ,  $P_3$  are respectively the test result, theoretical result by Eq. (13) and the theoretical result of load-bearing capacity for the specimen by Nakano *et al.* (2003).

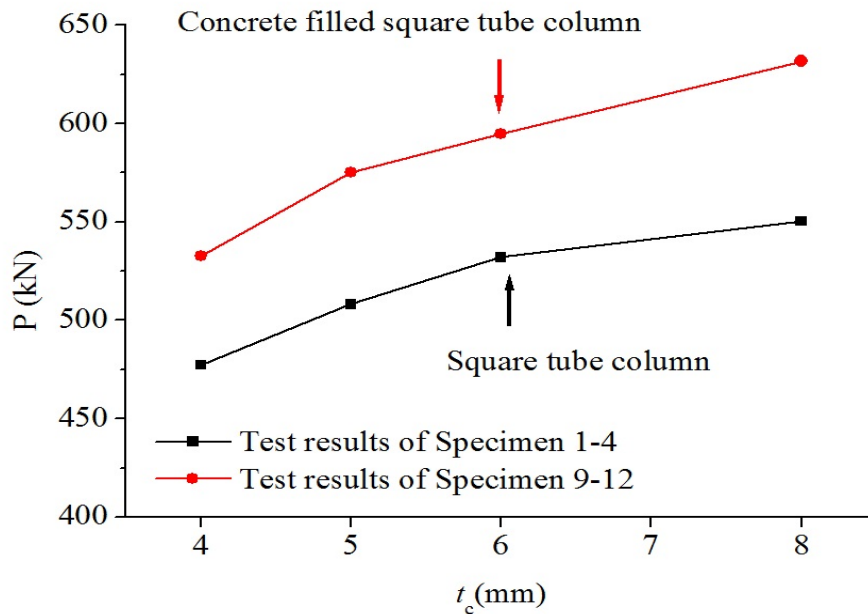


Fig. 12 Load-bearing capacity of specimen with filled concrete

feasible. As shown in Fig. 11 and Table 6, the test result of load-bearing capacity and the theory result by Eq. (13) are the same. The error of the theory result by Eq. (13) is less than the result by the load-bearing capacity derived by the yield line theory presented by Nakano *et al.* (2003). According to Fig. 12 and Table 7, the load-bearing capacity of the joints with concrete filled in the tube will increase by 10%~15%. The theoretical result of the joint load-bearing capacity by Eq. (13) is less than the test result, and the test result is approximately 1.2 times of the theoretical result. The error of the theoretical result by Eq. (13) is still less than the result of the load-bearing capacity based on yield line theory presented by Nakano *et al.* (2003). Therefore it is shown that the load-bearing capacity of the joints for H-shaped beam to concrete filled square tube column connection is larger than that of the joints for H-shaped beam to square tube column connection by 10% to 15%.

Table 7 Comparison of the load-bearing capacity of specimens with concrete filled

$t_c^*$ (mm)	$P_1$ (kN)	$P_2$ (kN)	$P_3$ (kN)	$P_4$ (kN)	$P_1/P_2$	$P_1/P_3$	$P_1/P_4$
4	532.9	477.3		432.2	1.116	1.075	1.233
5	575.2	508.2	495.6	436.3	1.132	1.161	1.318
6	594.6	532.0		445.9	1.118	1.200	1.334
8	631.7	550.4		465.0	1.148	1.275	1.359

\* $t_c$  is thickness of square tube column;  $P_1$  is test result of load-bearing capacity of the specimen with filled concrete;  $P_2$  is test result of load-bearing capacity of the specimen without filled concrete;  $P_3$  is theoretical result of the specimen by Eq. (13);  $P_4$  is the theoretical result of the specimen by Nakano *et al.* (2003).

Table 8 Stress at measuring point of the specimen

Specimen	$\sigma_1$ (N/mm <sup>2</sup> )	$\sigma_2$ (N/mm <sup>2</sup> )	$\sigma_3$ (N/mm <sup>2</sup> )
1	310.92	31.14	35.11
2	311.36	54.74	17.60
3	315.14	49.47	33.96
4	333.82	65.01	49.03
5	336.59	78.02	55.41
6	299.79	60.98	51.65
7	301.40	73.07	38.93
8	303.41	98.76	30.66
9	300.81	36.55	35.40
10	319.78	91.32	49.23
11	317.28	63.15	65.48
12	305.11	55.50	63.01

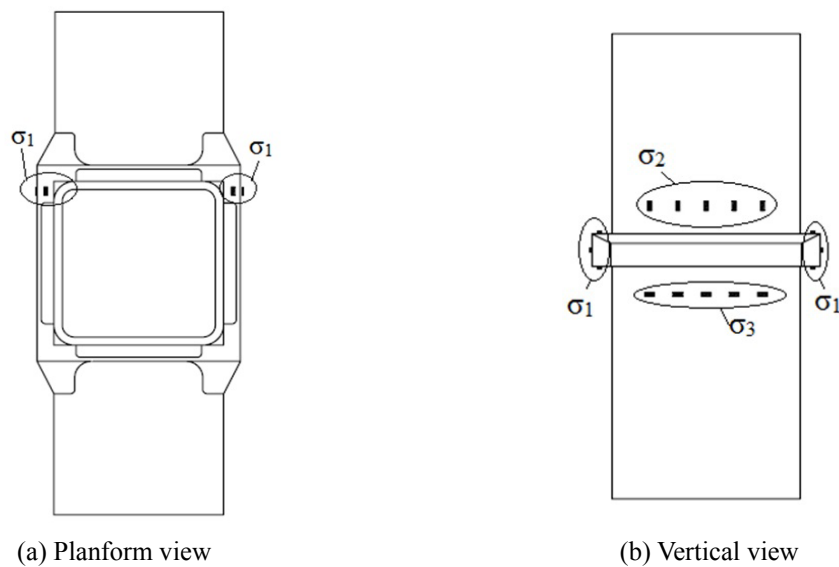


Fig. 13 Arrangement of measuring point for stress value

#### 4.2 Stress distribution

During the loading process in the test, the stress of the ring of stiffener significantly increases while the stress for the wall of square tube column increases a little. The stress of the ring of stiffener is greater than the stress of the wall of square tube column. To study the load transfer mechanism and the load distribution of the joints, the stress for each component of the joint is listed in Table 8 when the joint reaches the yield point. The stress of the ring of stiffener ( $\sigma_1$ ) and the stress of the wall of square tube column ( $\sigma_2$ ,  $\sigma_3$ ) are measured on the surface away from the welding connection to avoid the welding influence. The arrangement of measuring point for the stress is shown in Fig. 13.

As shown in Table 8, when the force on the joint reaches the yield load, the stress of the ring of stiffener  $\sigma_1$  is significantly higher than the stress of the wall of square tube column. It is proved that the cast steel stiffener bear most of force when the joint bears the bending moment. The load transfer mechanism is also conformed. The load-bearing capability of the joints depends on the cast steel stiffener. The test result consists with the load-bearing capacity theory based on the deformation compatibility condition well.

### 5. Conclusions

Monotonic tensile experiments are conducted in order to acquire the load transfer mechanism and load-bearing capability of cast steel joints for H-shaped beam to square tube column connection. Conclusions can be drawn base on the test result combined with the load-bearing capacity theory.

- The tensile bearing capacity of the cast steel joints for beam-column connection depends on the ring of cast steel stiffener. The tensile fracture happens at the ring of the cast steel stiffeners when the joint fails. The thickness of square tube column has little influence on the bearing capacity of the joint. The square tube column buckles while the joint without concrete filled, but the strength failure happens for the joint with concrete filled.

- The load transfer mechanism and mechanical characteristics of cast steel joints for H-shaped beam to square tube column can be acquired by the load-bearing capacity theory based on the deformation compatibility condition.

- It is shown that the load-bearing capacity of the joints for H-shaped beam to concrete filled square tube column connection is larger than that of the joints for H-shaped beam to square tube column connection by 10% to 15%.

- The length of welding connection between square tube column and cast steel stiffener has little influence on the load-bearing capacity of the cast steel joint.

### Acknowledgments

This research project is supported by the National Natural Science Foundation of China (No. 51178307, 51268054), Program for Tianjin Construction System Science Technology Development of China (No. 2013-35) and Tianjin Natural Science Foundation of China (No. 13JCQNJC07300). Support from the funding agency above is gratefully acknowledged.

## References

- Ciutina, A.L. and Dubina, D. (2006), "Seismic behaviour of steel beam-to-column joints with column web stiffening", *Struct. Eng. Mech.*, **6**(6), 493-512.
- Design code (2001), *Guide of design and construction of "HIBLADE process" of Hitachi*, Tokyo. (in Japanese)
- Han, Q.H., Liu, M.J. and Lu, Y. (2015), "Mechanical behavior analysis of cast steel joints for H-shaped beam to square tube column", *Journal of Tianjin University, Science and Technology*. (in Chinese) (in press).
- Kimura, J. and Matsui, C. (2005), "Structural characteristics of H-shaped beam-to-square tube column connection with vertical stiffeners", *Int. J. Steel Struct.*, KSSC, **5**(2), 109-117.
- Morino, S. and Tsuda, K. (2003), "Design and construction of concrete-filled steel tube column system in Japan", *Earthq. Eng. Eng. Seismol.*, **4**(1), 51-73.
- Nakano, K., Kitano, T. and Yoshinaga, K. *et al.* (2003), "Development of "HIBLADE process" with external stiffener rings using cast steel", *Hitachi Metals Technical Review*, **19**, 67-70. (in Japanese)
- Rong, B., Chen, Z., Zhang, R., Fafitis, A. and Yang, N. (2013), "Experimental and analytical investigation of the behavior of diaphragm-through joints of concrete-filled tubular columns", *J. Mech. Mater. Struct.*, **7**(10), 909-929.
- Shin, K.J., Kim, Y.J. and Oh, Y.S. (2008), "Seismic behaviour of composite concrete-filled tube column-to-beam moment connections", *J. Constr. Steel Res.*, **64**(1), 118-127.
- Skejjic, D., Dujmovic, D. and Androic, B. (2008), "Behaviour of welded beam-to-column joints subjected to the static load", *Struct. Eng. Mech.*, **29**(1), 17-35.
- Toellner, B.W., Watkins, C.E., Abbas, E.K. and Eatherton, M.R. (2015), "Experimental investigation on the seismic behavior of steel moment connections with decking attachments", *J. Constr. Steel Res.*, **105**, 174-185.
- Timoshenko, S. and Woinowsky-Krieger, S. (1959), *Theory of Plates and Shells*, McGraw-Hill, New York.
- Wang, J.F., Han, L.H. and Uy, B. (2009), "Behaviour of flush end plate joints to concrete-filled steel tubular columns", *J. Constr. Steel Res.*, **65**(4), 925-939.
- Wang J.F., Zhang, L. and Spencer, B. F. (2013), "Seismic response of extended end plate joints to concrete-filled steel tubular columns", *Eng. Struct.*, **49**, 876-892.
- Yin, Y., Han, Q.H., Bai, L.J., Yang, H.D. and Wang, S.P. (2009), "Experimental study on hysteretic behaviour of tubular N-joints", *J. Constr. Steel Res.*, **65**(2), 326-334.